FG.

12

TECHNICAL REPORT RR-76-1

LOW LOSS MODULATORS FOR INFRARED LASERS

G. A. Tanton and H. C. Meyer
Physical Sciences Directorate
US Army Missile Research, Development and Engineering Laboratory
US Army Missile Command
Redstone Arsenal, Alabama 35809

25 May 1976

Approved for public release; distribution unlimited.

U.S. ARMY MISSILE COMMAND
Redstone Arsenal, Alabama 35809

DISPOSITION INSTRUCTIONS

DESTROY THIS REPORT WHEN IT IS NO LONGER NEEDED. DO NOT RETURN IT TO THE ORIGINATOR.

DISCLAIMER

THE FINDINGS IN THIS REPORT ARE NOT TO BE CONSTRUED AS AN OFFICIAL DEPARTMENT OF THE ARMY POSITION UNLESS SO DESIGNATED BY OTHER AUTHORIZED DOCUMENTS.

TRADE NAMES

USE OF TRADE NAMES OR MANUFACTURERS IN THIS REPORT DOES NOT CONSTITUTE AN OFFICIAL INDORSEMENT OR APPROVAL OF THE USE OF SUCH COMMERCIAL HARDWARE OR SOFTWARE.

UNCLASSIFIED

SECURITY CLASSIFICATION OF THIS PAGE (When Data Entered)

REPORT DOCUMENTATION PAGE

READ INSTRUCTIONS BEFORE COMPLETING FORM

(14) 1. REPORT NUMBER: RR-76-1	2. GOVT ACCESSION NO.
3. RECIPIENT'S CATALOG NUMBER	
(6) 4. TITLE (and Subtitle): LOW LOSS MODULATORS FOR INFRARED LASERS	(9) 5. TYPE OF REPORT & PERIOD COVERED: Technical Report.
6. PERFORMING ORG. REPORT NUMBER: RR-76-1	
(10) 7. AUTHOR(s): G. A. Tanton and H. C. Meyer	8. CONTRACT OR GRANT NUMBER(s)
9. PERFORMING ORGANIZATION NAME AND ADDRESS: Commander, US Army Missile Command, ATTN: DRSMI-RR, Redstone Arsenal, Alabama 35809	10. PROGRAM ELEMENT, PROJECT, TASK AREA & WORK UNIT NUMBERS: DA Project 1W161102AH49, AMCMS Code 611102.11.H4900
11. CONTROLLING OFFICE NAME AND ADDRESS: Commander, US Army Missile Command, ATTN: DRSMI-RPR, Redstone Arsenal, Alabama 35809	(11) 12. REPORT DATE: 25 May 1976 (12) 20 p.
	13. NUMBER OF PAGES: 19
(16) 14. MONITORING AGENCY NAME & ADDRESS (if different from Controlling Office): DA-1-W-161102-AH-49	15. SECURITY CLASS. (of this report): UNCLASSIFIED
	15a. DECLASSIFICATION/DOWNGRADING SCHEDULE

16. DISTRIBUTION STATEMENT (of this Report)

Approved for public release; distribution unlimited.

17. DISTRIBUTION STATEMENT (of the abstract entered in Block 20, if different from Report)

18. SUPPLEMENTARY NOTES

19. KEY WORDS (Continue on reverse side if necessary and identify by block number)

Magneto-optical spectroscopy
Plane-of-polarization curves

20. ABSTRACT (Continue on reverse side if necessary and identify by block number)

This report shows how magneto-optical properties of bound state transitions may be used to design components significantly more efficient than conventional designs for infrared and submillimeter wavelengths. It is shown that magneto-optical spectroscopy can also provide information about basic parameters of a system not easily obtainable by other means.

DD FORM 1 JAN 73 1473 EDITION OF 1 NOV 65 IS OBSOLETE

400625

UNCLASSIFIED

SECURITY CLASSIFICATION OF THIS PAGE (When Data Entered)

CONTENTS

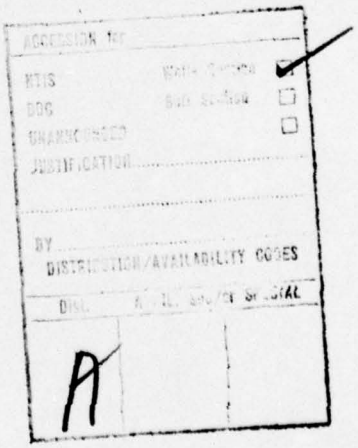

ACKNOWLEDGEMENTS

The authors thank Dr. Zoltan Kiss for $CaF_2:Dy^{2+}$ specimens and acknowledge helpful discussions with Dr. S. S. Mitra, Dr. J. D. Stettler, and Mr. R. A. Shatas. We also thank Mr. J. E. Williams for his able assistance with the experiments.

I. INTRODUCTION

High power lasers which operate in the infrared (IR) spectral region are used in advanced systems now being researched and developed by the Army. There is a critical need for efficient components, e.g., frequency shifters, spectral filters, modulators, and rotators to realize the full potential of these lasers. Conventional modulator materials such as KDP operate satisfactorily in the visible wavelengths but are ineffective at IR wavelengths for use in high power IR systems. The term modulator is used here in the broad sense to mean a device by which the beam can be manipulated or controlled. Thus a rotator is a special type of modulator. Among the most promising conventional modulator materials in the IR are GaAs and CdTe which have been investigated at 10.6 μ. These materials have shortcomings for amplitude modulation and large index phase modulation applications. Due to insufficient linearity, small linear and angular apertures, and high absorption, they are unsuitable for use in powerful CO_2 laser systems to which the Army is committed. These applications of materials utilize their bulk properties.

II. THEORETICAL CONSIDERATIONS

A radically different approach to the problems of designing low loss modulators for the IR is shown here. This approach has high merit. In this technique the Faraday rotation of Zeeman split energy levels in the material, due either to doping or the molecular structure of the material, is used. To see how this can be done, the complex index of refraction $\hat{n}$ which describes optical properties of a material is considered. The real part n of $\hat{n}$ is associated with the dispersion; the imaginary part K is a function of the absorption α

$$K = \frac{c}{2\omega} \alpha \tag{1}$$

where ω is the angular frequency of light and c is the speed of light in a vacuum. Thus, for right circularly polarized light (+) or left circularly polarized light (-)

$$\hat{n}_{\pm} \approx n_{\pm} - i K_{\pm} \quad . \tag{2}$$

Faraday rotation Φ, the angle of rotation of the plane of polarization of plane polarized light, is given by

$$\theta = \frac{\omega}{2c} (n_+ - n_-) \quad . \tag{3}$$

Figure 1 illustrates how magneto-optical properties of bound state transitions result in a splitting of the absorption line, which gives rise to Faraday rotation.

Electric dipole transitions which change the magnetic quantum number M_J by +1 or -1 correspond to right- or left-circular polarization, respectively, as represented in Figure 1. The upper state degeneracy, removed by an external magnetic field, B, is indicated together with the resulting absorption-line components, which are shown as a function of photon energy, E. Since the absorption $\alpha(E)$ and angle of rotation $\theta(E)$ of the plane of polarization are functions of the imaginary and real part of the complex index of refraction respectively, $\theta(E)$ can be calculated from $\alpha(E)$ by use of the dispersion relation [1]

$$\theta_{\pm}(E) = \frac{E^2}{2\pi} \int_0^{\infty} \frac{\alpha_{\pm}(E')dE'}{E'(E^2 - E'^2)} \quad . \tag{4}$$

$\theta(E) = \theta_+(E) - \theta_-(E)$ has been calculated from assumed shapes of $\alpha_{\pm}(E)$ by numerically integrating Equation (4). These computed values are compared with the measured values [2] of Faraday rotation due to $^7F_0 \rightarrow {}^5D_1$ transitions in $CaF_2:Sm^{2+}$. Excellent agreement between calculated and measured rotation spectra was obtained, as is shown in Figure 2 with Gaussian-shape absorption components $\alpha_+(E)$ and $\alpha_-(E)$. Lorentzian shapes of the same width were also tried and did not fit as well. The Faraday-rotation spectrum in Figure 2(b) was calculated by normalizing a Gaussian line shape to the measured peak absorption coefficient. The absorption coefficient $\mu_{\pm}$ is plotted with a dotted line in Figure 2(b) and is related to $\alpha_{\pm}$ by $\mu_{\pm} = n\alpha_{\pm}$, where n is the bulk index of refraction, taken here to be 1.45. Although a closer fit between calculated and measured curves could have been obtained by adjusting line-shape parameters, agreement was considered already adequate to establish the validity of the computational procedure used.

The rotation $\theta(E)$, computed for two different separations of $\alpha_+(E)$ and $\alpha_-(E)$, is shown in Figures 3a and 3b for Gaussian-shape components that have equal amplitudes and half widths. At a position E_o, $\theta(E)$ decreases less rapidly than $\alpha(E)$ as the separation between the two components increases. The computed ratio $\alpha(E_o)/\theta(E_o)$, plotted as a function of component separation δ, in units of half width, is shown in Figure 3c for the spectral region between $\alpha_+(E)$ and $\alpha_-(E)$, where $\alpha(E) = \alpha_+(E) + \alpha_-(E)$. It can be seen that for $\delta \geq 5$, $\alpha(E_o)/\theta(E_o)$ is very small compared to its initial value.

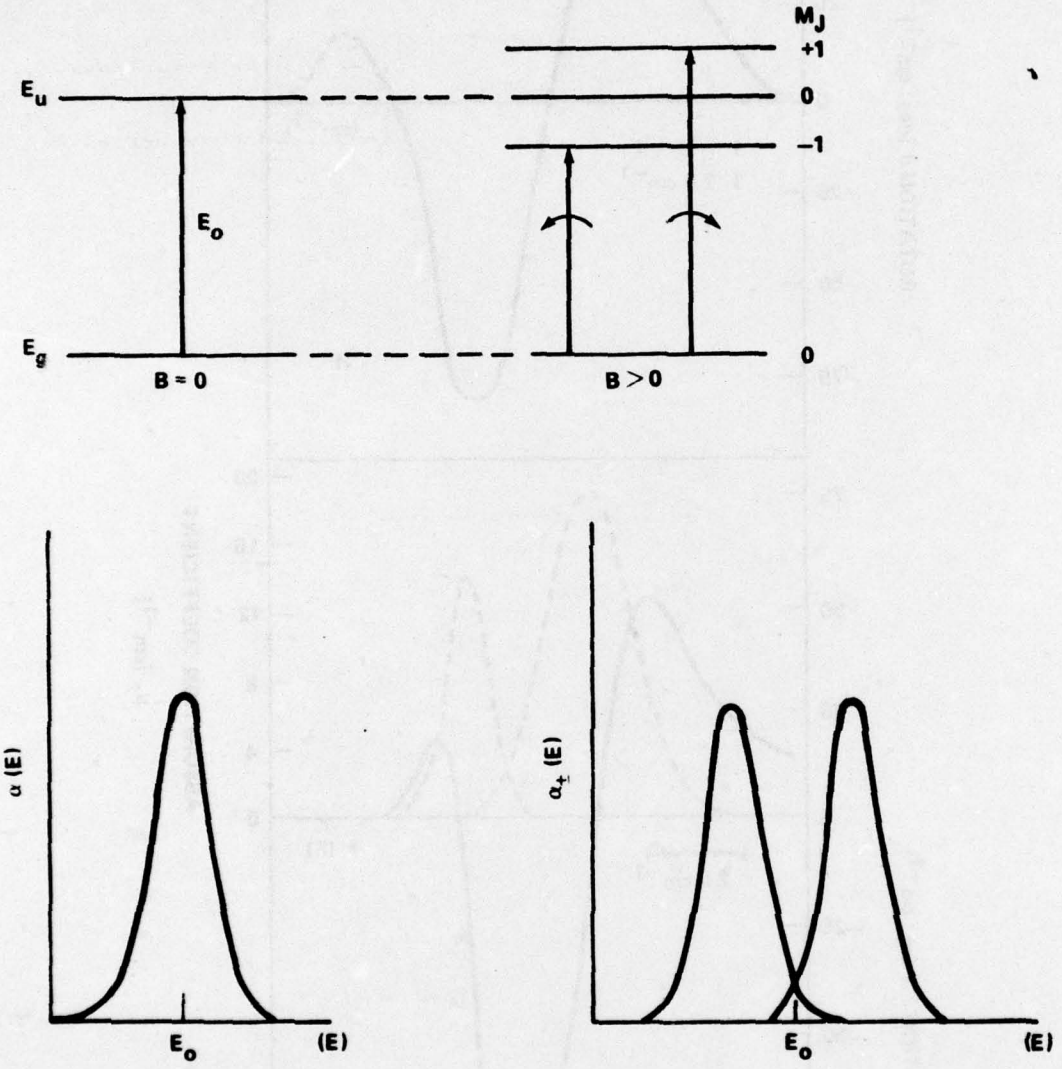

Figure 1. Upper-state energy level E_u split by an external magnetic field B and resulting absorption line components as a function of photon energy E.

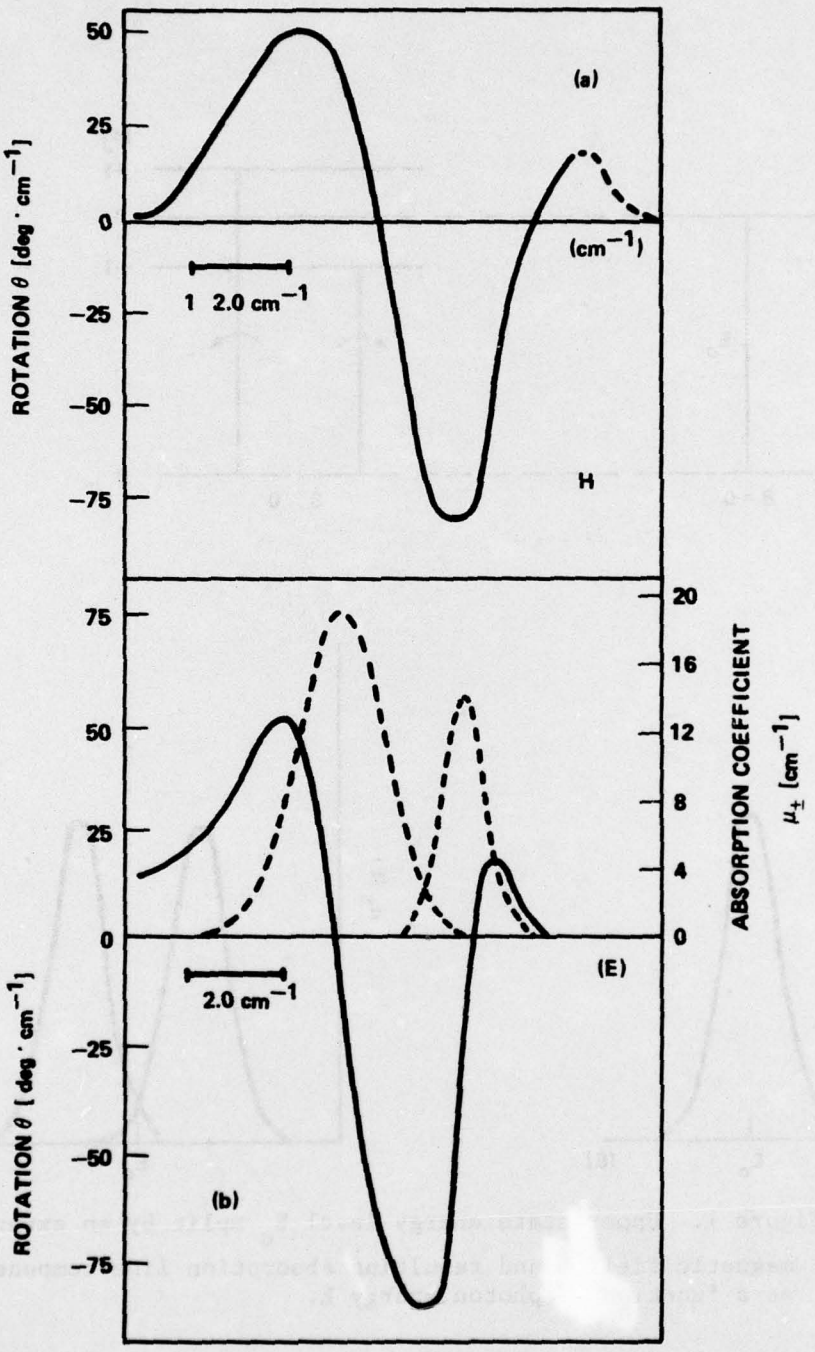

Figure 2. Measured rotation spectrum (a) of $^1F_0 - {}^5D_1$ transition in $CaF_2:Sm^{2+}$ at 4.3 k, B = 60 kG. Rotation spectrum (solid line) calculated (b) from Gaussian-shape absorption components (dotted lines) normalized to the measured peak absorption coefficient.

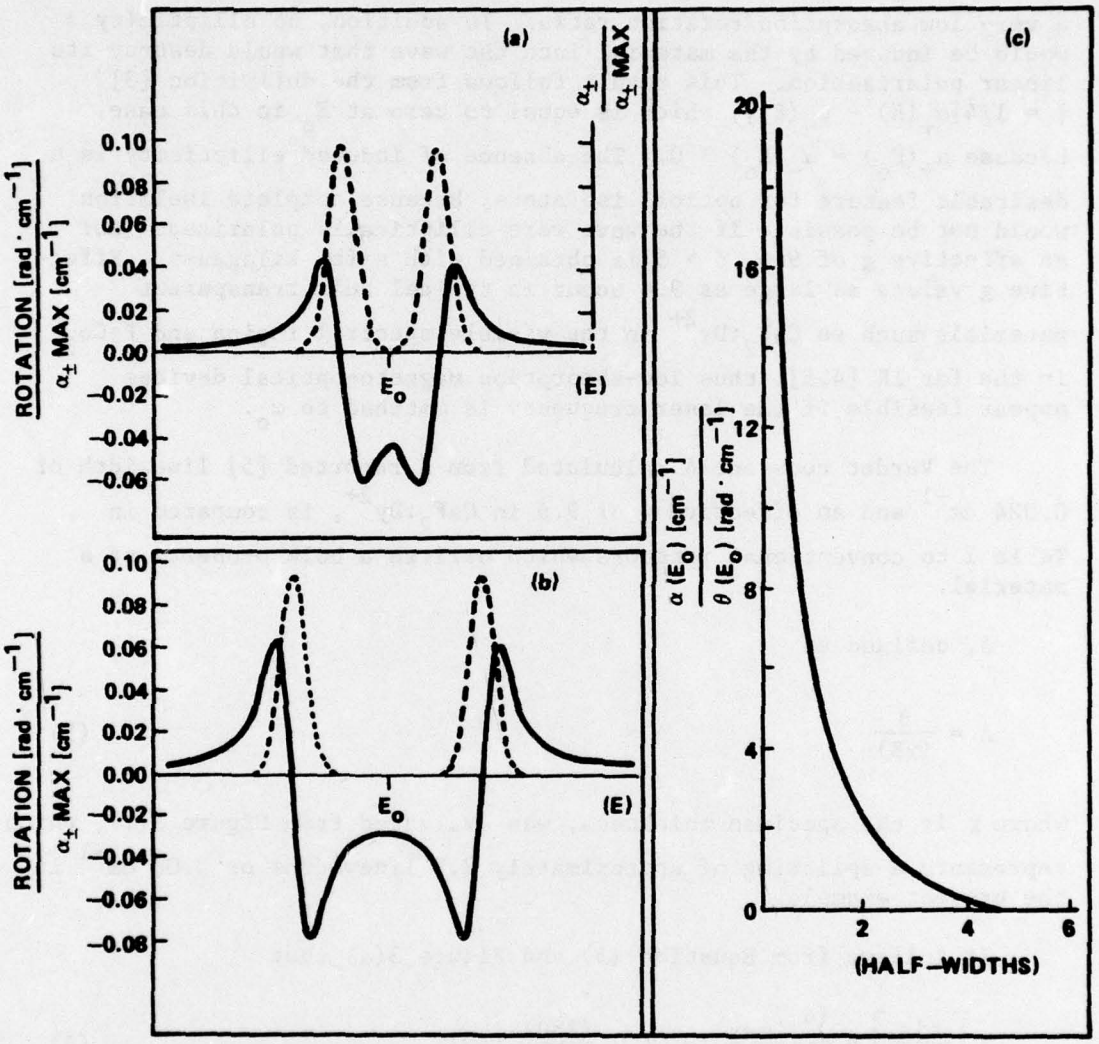

Figure 3. Rotation spectra represented by the solid line in (a) and (b) computed for different separations δ of $\alpha_+(E)$ and $\alpha_-(E)$, represented by dotted lines which have Gaussian shapes. Numbers shown along the ordinate must be multiplied by the maximum values of $\alpha_\pm$ to obtain rotation. (c) Computed ratio $\alpha(E_0)/\theta(E_0)$ as a function of component separation.

At a separation of approximately 5 half widths, a wave with frequency ω_o could be expected to propagate through the material with a very low absorption/rotation ratio. In addition, no ellipticity ϕ would be induced by the material into the wave that would destroy its linear polarization. This result follows from the definition [3] $\phi = 1/4[\alpha_+(E) - \alpha_-(E)]$, which is equal to zero at E_o in this case, because $\alpha_+(E_o) = \alpha_-(E_o) \approx 0$. The absence of induced ellipticity is a desirable feature for optical isolators, because complete isolation would not be possible if the wave were elliptically polarized. For an effective g of 9.6, $\delta > 5$ is obtained with a few kilogauss. Effective g values as large as 9.6 occur in typical bulk transparent materials such as $CaF_2:Dy^{2+}$ in the visible spectral region and $FeCo_3$ in the far IR [4,5]; thus low-absorption magneto-optical devices appear feasible if the laser frequency is matched to ω_o.

The Verdet constant Λ calculated from a reported [5] linewidth of 0.024 cm^{-1} and an effective g of 9.6 in $CaF_2:Dy^{2+}$, is compared in Table 1 to conventional rotators which utilize a bulk property of a material.

Λ, defined as

$$\Lambda = \frac{\theta}{(\chi B)} \tag{5}$$

where χ is the specimen thickness, was evaluated from Figure 3(a), which represents a splitting of approximately 2.5 linewidths or 0.06 cm^{-1} in the present example.

It follows from Equation (5) and Figure 3(a) that

$$\Lambda \left[\frac{\text{min}}{\text{cm}\cdot\text{G}}\right] = \frac{(\alpha_\pm)_{\text{max}}}{B} (0.042) \frac{(180)}{\pi} (60) \quad . \tag{6}$$

The required magnetic field B = 135 G was found from the line-splitting rate of 0.45 cm^{-1}/kG. It is assumed that $(\alpha_\pm)_{\text{max}} = 10\ cm^{-1}$ and from Equation (3) it follows that $\Lambda = 10$ min/cm·G.

The calculated insertion loss follows from the Gaussian line shape of the components and the maximum value of $\alpha_\pm(E)$. Thus

TABLE 1. MAGNETO-OPTICAL CONSTANTS OF MATERIALS

	T (°K)	Verdet Constant (min $G^{-1} \cdot cm^{-1}$)	λ (microns)	Insertion Loss (dB)
TAG [1]	300	1.27	0.514	0.4
Corning 8363 [3]	300	0.1	0.61	1.0
InSb	77	0.66	10.6	2.0
$CaF_2:Dy^{2+}$ (Calculated)	10	10.0	2.360	0.0

$$\alpha_{\pm}(E_o) = (\alpha_{\pm})_{max} e^{-5^2} \approx 10^{-10} \quad [cm^{-1}] \text{ at } \delta = 5 \quad . \tag{7}$$

Only absorption due to transitions between bound states is included in this calculation.

A low loss IR rotator has been designed based on the preceding analysis applied to data of Blum et al. for NO [6].

III. DEVICE APPLICATION

Laser radiation of wavelength 5.26 μ is directed from left to right in Figure 4 through a polarizer onto the rotator. An absorption line in the rotator is split into two components by the application of an external magnetic field from the superconducting solenoid. The strength of the magnetic field is adjusted so that the light of frequency ω_o passes through the rotator at a spectral position between the split absorption components. Thus, very little absorption will take place and the plane of polarization will be rotated without introducing ellipticity into the beam polarization. The length of the rotator is chosen to cause a 45° rotation. An adjustable heater and a thermocouple are provided to temperature tune and stabilize the rotator. After leaving the rotator, the light beam passes through the analyzer which is orientated with its plane of polarization coincident with that of the light beam. Thus, the light beam will pass through left to right but not in reverse, because light coming from the right in Figure 4 will be polarized by the analyzer at an angle of 45°. After passing through the rotator, an additional 45° rotation will occur; thus a light beam entering from the right will be polarized 90° to the polarizer and therefore will not be transmitted through it. The result is to isolate optically everything to the left of polarizer.

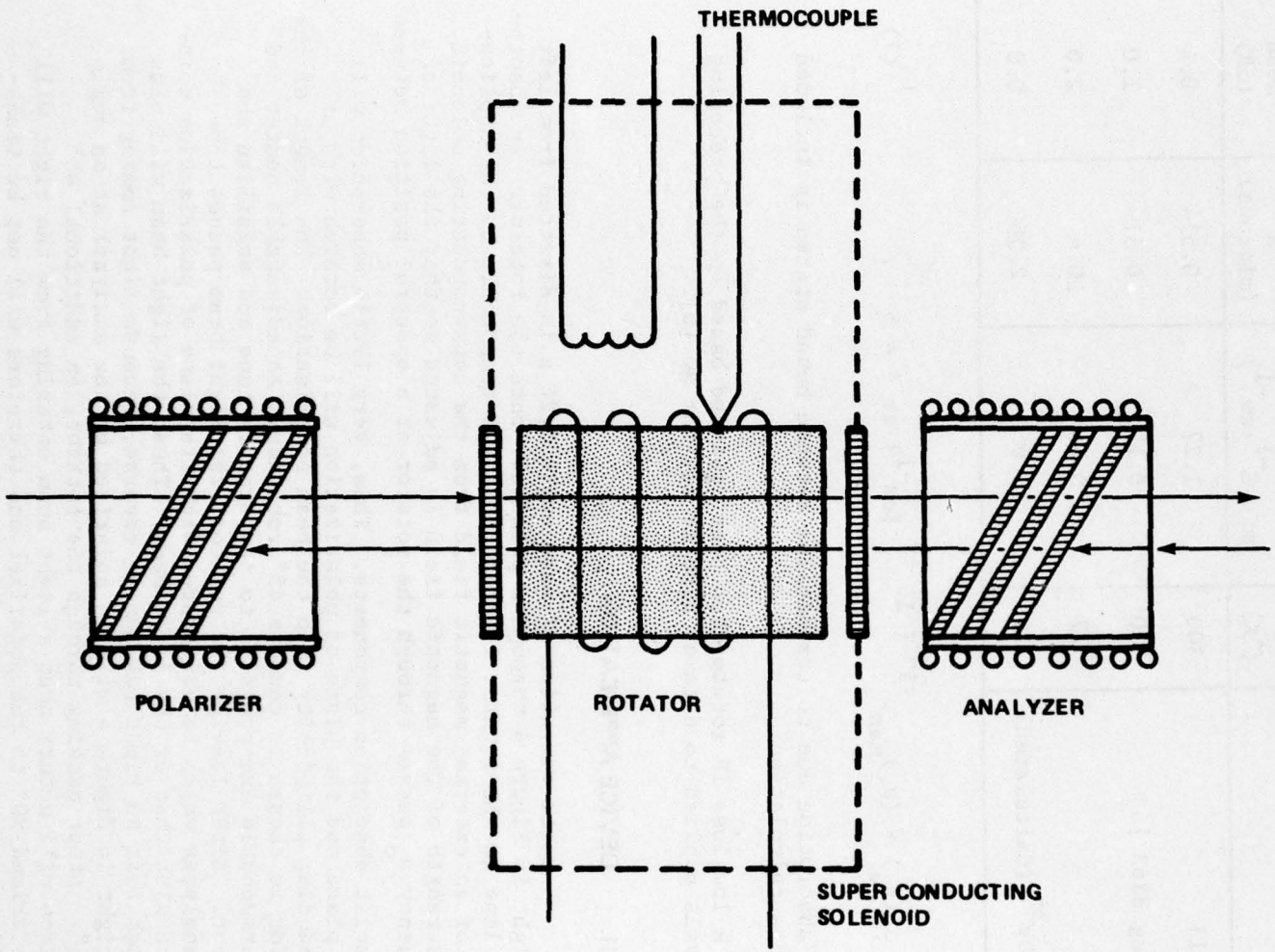

Figure 4. Isolator configuration.

For NO, using values reported by Blum et al. [6] (left side of Table 2), the design parameters for an isolator are determined (right side of Table 2).

TABLE 2. DESIGN PARAMETERS FOR NO ROTATOR

	Blum et al. [6]	Calculated Design Parameters
B	30 kg	100 kg
Separation of components in halfwidths	2.0	5
Rotation per unit length	5.5°/cm	2.4°/cm
Cell length for 45° rotation		18.8 cm
Pressure	3 torr	3 torr
Rotator absorption		$\sim 10^{-10}$ cm^{-1}

Correction for a finite laser linewidth was found to be negligible for a width of 5, the maximum value assumed.

IV. DIAGNOSTIC APPLICATIONS

To determine their suitability as modulators, it is necessary to investigate basic magneto-optical properties of bound state transitions within the materials. The technique [7,8] developed allows the determination of such parameters as g values from the Faraday rotation spectrum which previously had been obtained from much more difficult high resolution absorption measurements [9].

Figure 5 shows that absorption components due to transitions from ^7F_o to $^5D_{+1}$ and $^5D_{-1}$ levels were not resolved with the minimum usable spectral slit width of 0.6 cm^{-1}. Faraday rotation allows $^5D_{\pm 1}$ level splitting to be determined accurately (Figure 6). The Faraday rotation spectrum was resolved into two dispersion curves, n_+ and n_-.

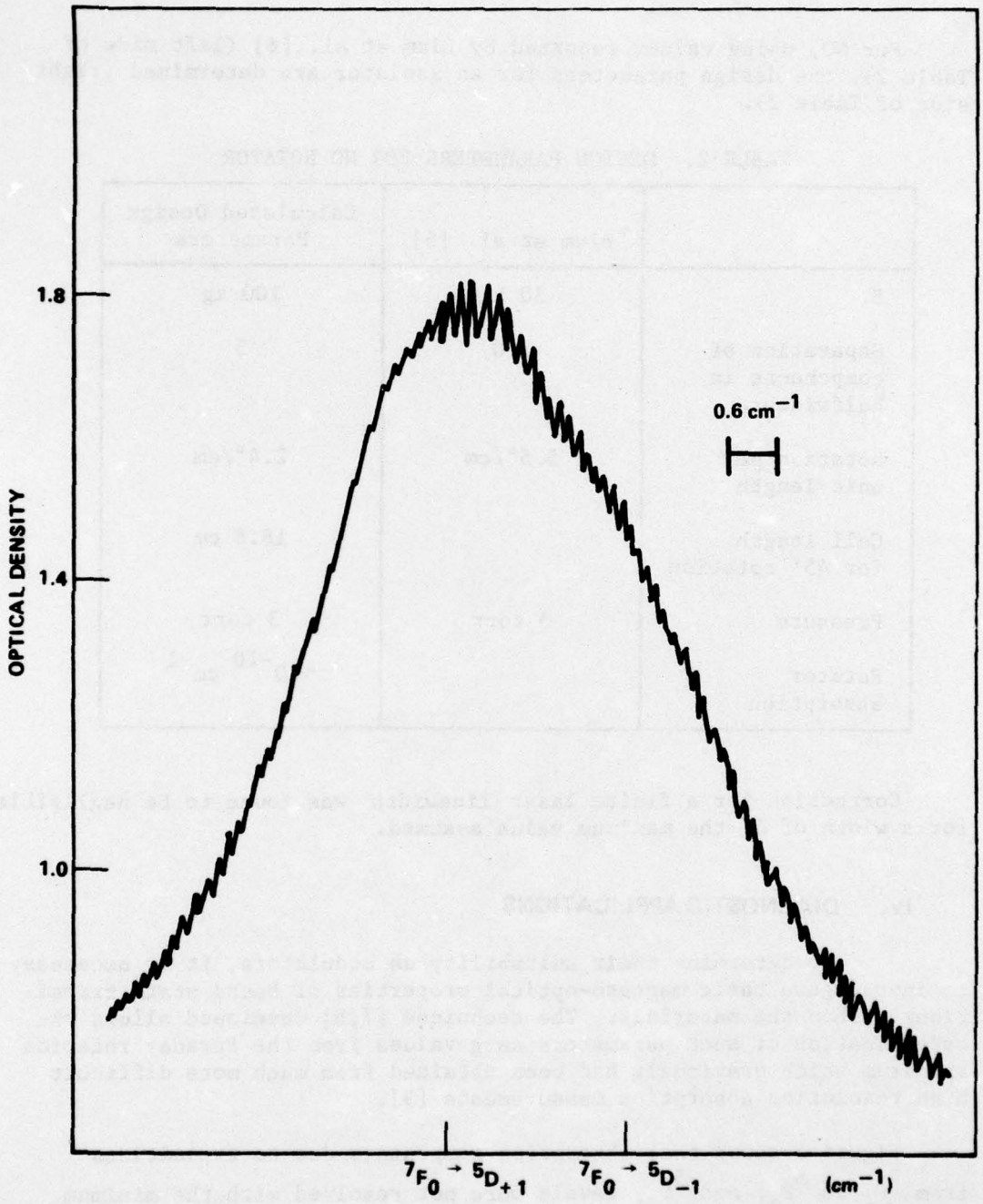

Figure 5. Absorption due to $^7F_0 \rightarrow {}^5D_{\pm 1}$ transitions in $CaF_2:Sm^{2+}$ at liquid-helium temperatures in a 60 kG magnetic field.

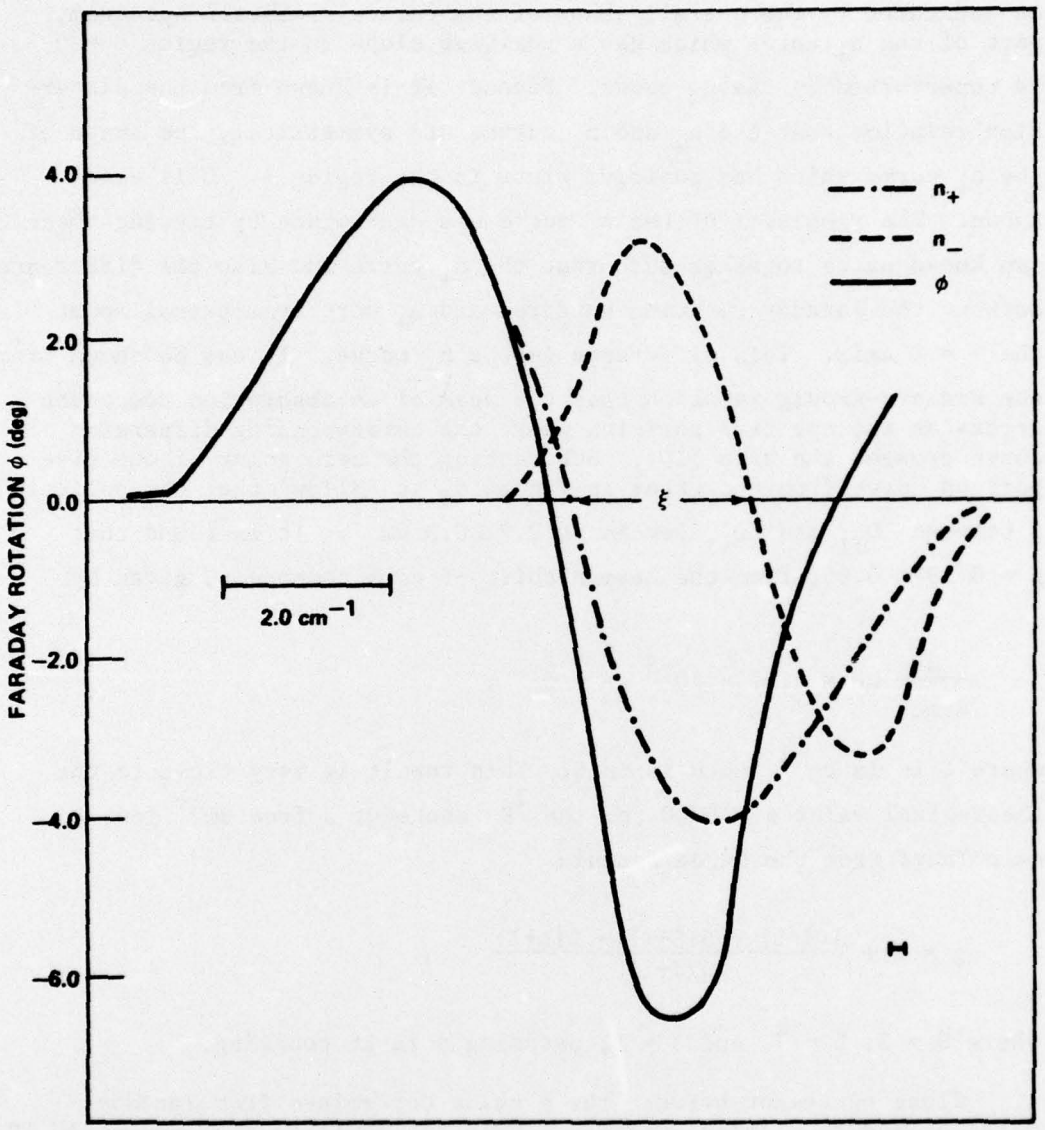

Figure 6. Faraday rotation of $^7F_0 \rightarrow {}^5D_{\pm 1}$ transition in $CaF_2:Sm^{2+}$. ξ is the separation between $^5D_{+1}$ and $^5D_{-1}$ components due to an external 60 kG field.

As indicated by the overall shape of the Faraday rotation spectrum, part of the n_+ curve which has a positive slope in the region $\theta > 0$ is unperturbed by the n_- curve. Because it is known from the dispersion relation that the n_+ and n_- curves are symmetrical, the shape of the n_+ curve which has positive slope in the region $\theta < 0$ is also known. The remainder of the n_+ curve was determined by fitting these two known parts together such that the n_+ curve and also the difference between the Faraday rotation spectrum and n_+ were symmetrical about the $\theta = 0$ axis. This difference is the n_- curve. It can be shown from the Kramers-Kronig relation that the peak of an absorption component occurs at the spectral position where the corresponding dispersion curve crosses the axis [10]. Subtracting the zero point of one dispersion curve from the other in Figure 6, it follows that the splitting ξ between $^5D_{+1}$ and $^5D_{-1}$ levels is 2.2 ± 0.3 cm^{-1}. It is found that $g = 0.39 \pm 0.03$, from the Zeeman shift of each component, given by

$$\frac{e}{4\pi mc^2} gH = 4.67 \times 10^{-5} gH = \frac{\xi}{2} \quad ,$$

where ξ is in cm^{-1} and H is in G. This result is very close to the theoretical value $g = 0.40$ for the $^7K_4$ state of a free Sm^{2+} ion, calculated from the Landé formula

$$g = 1 + \frac{J(J+1) + S(S+1) - L(L+1)}{2J(J+1)} \quad ,$$

where $S = 3$, $L = 7$, and $J = 4$, assuming pure LS coupling.

Close agreement between the g value determined from Faraday rotation and that calculated for a free ion supports the assumption of Kaiser et al. [11] that these transitions in $CaF_2:Sm^{2+}$ occur within highly shielded shells (e.g., f shells).

Results from Faraday rotation are consistent with high-resolution absorption data reported by Zakharchenya and Ryskin [9], although a somewhat lower $g = 0.31$ was found by Margerie from magnetic dichroism studies [12]. This technique has been extended to treat more complicated energy level schemes such as the F-center in BaF_2.

This extension of the computational method used here was applied to the accepted energy level scheme for an F-center in a alkali halide lattice to determine the type of defect responsible for absorption bands in the more complex alkaline earth fluorides, e.g., BaF_2, CaF_2, and SrF_2. Experimentally determined Faraday rotation spectra and those computed from the model agree closely in the overall features for low temperature X-ray irradiated BaF_2. As before, Gaussian curves gave the best fit. With the aid of this analysis, it was found that the accepted energy level scheme for an F-center in a lattice with O_h symmetry is adequate to explain the more complex case of a single electron trapped in a lattice with T_d symmetry.

V. CONCLUSIONS

Calculated and experimentally determined plane-of-polarization curves presented demonstrate that magneto-optical properties of transitions between degenerate energy levels may be used to design low loss components for laser systems over the ultraviolet (UV) to far-IR spectral region. For devices such as optical rotators and modulators, magneto-optical properties of discrete-energy-level transitions offer significant advantages over bulk properties which are used in conventional designs.

In addition to novel device applications, it has been shown how magneto-optical spectroscopy can also provide information about basic parameters of a system, not easily obtainable by other means.

REFERENCES

1. Healy, W. P. and Power, E. A., Am. J. Phys. 42, 1070 (1974).

2. Tanton, G. A., J. Opt. Soc. Am. 65, 95 (1975).

3. Starostin, N. V. and Feofilov, P. P., Usp. Fiz. Nauk 97, 621 (1969). [Sov. Phys.-Usp. 12, 252 (1969)].

4. Prinz, G. A., Foster, D. W., and Lewis, J. L., Phys. Rev. 8, 2155 (1973).

5. Pressly, Robert J. and Wittke, James P., IEEE J. Quant. Elect. 3, 116 (1967).

6. Blum, F. A., Nill, K. W., and Strauss, A. J., J. Chem. Phys. 58, 4968 (1973).

7. Tanton, G. A. and Jason, Andrew J., Opt. 12, 897 (1973).

8. Smith, J. Lynn, Tanton, G. A., and Gamble, W. L., Appl. Opt. 13, 1451 (1974).

9. Zakharchenya, B. P. and Ryskin, A. Ya., Opt. Spectrosk. 13, 875 (1962) [Opt. Spectrosc. 13, 501 (1962)].

10. Starostin, N. V. and Feofilov, P. P., Usp. Fiz. Nauk 97, 621 (1969) [Sov. Phys.-Usp. 12, 252 (1969)].

11. Kaiser, W., Garrett, C. G. B., and Wood, D. L., Phys. Rev. 123, 766 (1961).

12. Margerie, J., Physica 33, 238 (1967).

DISTRIBUTION

	No. of Copies
Defense Documentation Center Cameron Station Alexandria, Virginia 22314	12
Commander US Army Materiel Development and Readiness Command	
ATTN: DRCRD	1
DRCDL	1
5001 Eisenhower Avenue Alexandria, Virginia 22333	
DRSMI-FR, Mr. Strickland	1
-LP, Mr. Voigt	1
-R, Dr. McDaniel	1
Dr. Kobler	1
-RBD	3
-RPR (Record Set)	1
(Reference Copy)	1
-RR, Mrs. Davis	5
-RRD, Mr. Tanton	20